High-order Čerenkov laser gain

I. J. Owens and J. H. Brownell
Department of Physics and Astronomy, Dartmouth College, Hanover, New Hampshire 03755-3528
(Received 5 December 2002; published 20 March 2003)

Čerenkov free-electron lasers have primarily operated on the fundamental guided mode of the dielectric waveguide. Higher-order generation would allow short wavelength emission in a relatively large scale resonator. In comparison to the fundamental mode, we find that gain on higher-order modes can be significant in a planar geometry. This analysis is presented with a discussion of practical limits.

DOI: 10.1103/PhysRevE.67.036611 PACS number(s): 41.60.Cr, 42.60.Da, 07.57.Hm

I. INTRODUCTION

Although there exists a number of light sources that are capable of producing electromagnetic radiation over a wide range of frequencies, there remains a gap in coverage in the far-infrared (FIR) spectral range. The Čerenkov free-electron laser (CFEL) is an interesting candidate for a tunable source of short wavelength radiation that shows ability to fill this chasm in the spectrum. The CFEL has been investigated both experimentally [1,2] and theoretically [3–6], but little is known about the interaction of the electron beam with higher-order modes. The majority of the theoretical papers published up to this point have focused on the properties of the fundamental guided mode. One exception is with Shiozawa and Kondo who published a paper on mode analysis and broadly concluded that the spatial gain is reduced on higher orders [4,5]. The purpose of this paper is to detail and examine the spatial gain on higher-order modes and control of the beam-dielectric gap that would allow for the production of far-infrared radiation with significant growth.

II. DISPERSION RELATION

The CFEL is essentially a dielectric waveguide driven by an adjacent electron beam. The current induced by the slow, guided Čerenkov mode generates a wave that grows exponentially. The mode wavelength is governed by the thickness of the dielectric. In the FIR region, this thickness is of the order of tens of microns, and so practical configurations entail supporting the dielectric on a substrate, typically conductive.

We consider here a simple planar geometry as shown in Fig. 1. The dielectric slab of strength ϵ is bounded below by a semi-infinite, perfect metal ground plane. A finite vacuum gap separates the dielectric slab and beam traveling parallel to the slab and vacuum exists above the beam. The system is symmetric in the transverse $\hat{\mathbf{y}}$ direction.

The unperturbed electron beam is collimated and monoenergetic, with velocity $\mathbf{v}=v\hat{\mathbf{z}}$, and fills the region $g<x<g+a$ uniformly with number density ρ. Electron motion is confined to the forward $\hat{\mathbf{z}}$ direction by an effectively infinite magnetic field. The beam therefore can be represented by an effective dielectric tensor derived from the linearized force and charge conservation equations,

$$\epsilon_{\text{beam}}=\hat{\mathbf{x}}\hat{\mathbf{x}}+\hat{\mathbf{y}}\hat{\mathbf{y}}+\epsilon_{\parallel}\hat{\mathbf{z}}\hat{\mathbf{z}}, \tag{1}$$

where

$$\epsilon_{\parallel}=1-\omega_p^2/\gamma^3(\omega-k_z v)^2, \tag{2}$$

the plasma frequency is defined by $\omega_p^2=4\pi\rho e^2/m$, and $\gamma=1/\sqrt{1-\beta^2}$ with $\beta=v/c$. Here, e and m refer to the electron charge and mass, while c is the speed of light.

The dispersion relation is developed from solutions of Maxwell's equations for the electric (**E**) and magnetic (**B**) fields, incorporating the beam-dielectric function above [Eq. (1)], and applying the appropriate boundary conditions at the four surfaces of the slab and beam. Given the rectilinear geometry, the fields can be conveniently decomposed into Fourier components. In each of the four distinct regions indicated in Fig. 1, express the longitudinal field component in the form

$$E_{zj}=(A_j^+ e^{ik_{xj}x}+A_j^- e^{-ik_{xj}x})e^{[i(k_z z-\omega t)]}, \tag{3}$$

with region index j ranging from one to four. We consider the transverse-magnetic (TM) mode only, so that $B_z=0$, and assume forward propagation (field amplitudes independent of y) for simplicity. By virtue of the diagonal anisotropy of the beam tensor, the wave vector must satisfy the wave equation

$$k_x^2+\epsilon_{\parallel}(k_z^2-\epsilon\omega^2)=0, \tag{4}$$

where it is understood that $\epsilon_{\parallel}=1$ outside the beam and $\epsilon=1$ outside the slab. The remaining field components are determined by the divergence and displacement current (D) equations

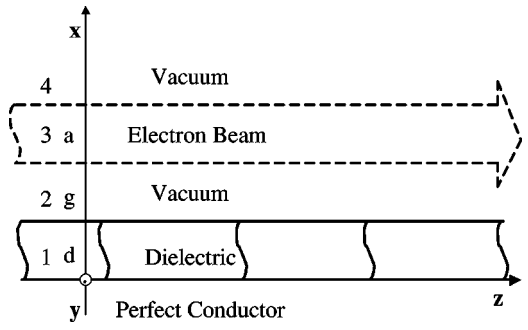

FIG. 1. Geometry of the dielectric resonator. The widths of the dielectric film, electron beam, and the gap between them are designated d, a, and g, respectively.

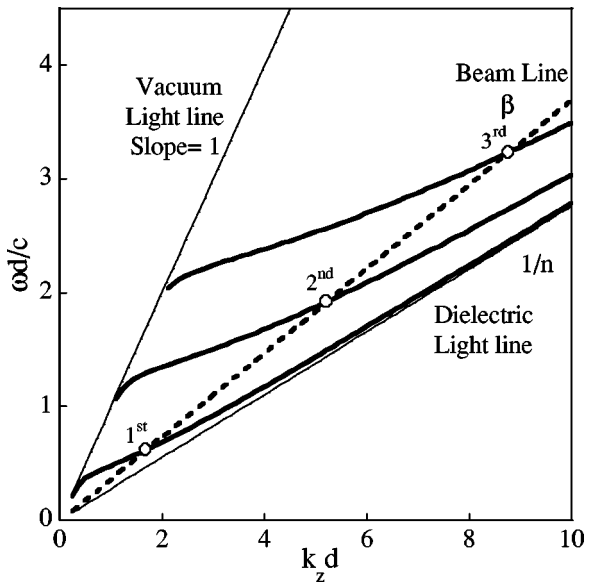

FIG. 2. First three operating points (open circles) of the CFEL determined by the intersection of the beam line (β=37) (heavy dotted line) with the TM film modes (heavy solid lines). The case for intrinsic GaAs (ϵ=13.1) is shown.

$$\partial_x E_{xj} = -ik_z \epsilon_\parallel E_{zj}, \tag{5}$$

$$k_z B_{yj} = (\epsilon\omega/c) E_{xj}. \tag{6}$$

By absorbing the electric current into the dielectric function, E_z and D_x are continuous, particularly at each interface between regions. Note that the boundary condition for B_{yj} is redundant to that of E_{xj}. The condition that the electric field must be zero within the perfectly conducting substrate forces, the tangential component of the electric field to vanish at $x=0$, and $A_1^- = -A_1^+$. At $x\to\infty$, the fields must remain finite. Since significant coupling occurs only when the field phase velocity matches the electron speed ($\omega \approx k_z v$, see Fig. 2), the field is evanescent above the beam. The condition $A_4^- = 0$ eliminates the growing term. The resulting set of six coupled linear equations can be reduced by Gaussian elimination to yield the dispersion relation $\Phi = 0$, where

$$\Phi(\omega, k_z, \omega_p) = \psi f_2 - f_3, \tag{7}$$

with

$$\psi = \frac{k_{x1}\tan(k_{x1}d)}{\epsilon q_o}, \tag{8}$$

$$f_2 = \left(\frac{1 + \frac{1}{\psi}\tanh(q_o g)}{1 + \psi \tanh(q_o g)} \right), \tag{9}$$

$$f_3 = \left(\frac{1 + \frac{1}{\sqrt{\epsilon_\parallel}}\tanh(qa)}{1 + \sqrt{\epsilon_\parallel}\tanh(qa)} \right). \tag{10}$$

The wave numbers in the normal direction have been defined in the dielectric, beam, and vacuum regions as $k_{x1} = \sqrt{\epsilon\omega^2/c^2 - k_z^2}$, $q = \sqrt{\epsilon_\parallel(k_z^2 - \omega^2/c^2)}$, and $q_o = \sqrt{k_z^2 - \omega^2/c^2}$, respectively.

One parameter can be eliminated from the dispersion relation by rendering the terms in Φ unitless. Given the slab thickness d is the only dimension in the absence of the beam, we normalize all lengths by d and frequencies by c/d. Then, all results can be simply scaled for any value of d.

For zero current ($\epsilon_\parallel = 1$), the familiar no-beam dispersion $\Phi = \psi - 1 = 0$ is obtained and has been treated by many authors [1,3,4,5]. The first three orders of the solution for this case are plotted in dark, solid lines in Fig. 2. The limit where the beam fills the half space above the slab ($g\to 0$, $a\to\infty$) produces $\Phi = \psi - 1/\sqrt{\epsilon_\parallel}$.

III. ANALYTIC GAIN EXPRESSION

The dispersion relation is transcendental and so does not yield an exact analytic solution. In order to develop an expression for CFEL gain, we introduce an approximate technique that assumes an electron beam with infinite thickness and low beam density ($\omega_p \ll \omega$) so that the dispersion relation can be Taylor expanded about the roots of the no-beam dispersion:

$$\Phi \approx \frac{\partial\Phi_n}{\partial\omega}(\omega - \omega_n) + \frac{\partial\Phi_n}{\partial k_z}(k_z - k_{zn}) + \frac{\partial\Phi_n}{\partial\omega_p^2}(\omega_p^2) = 0, \tag{11}$$

where it is given that $\Phi(\omega_n, k_{zn} = \omega_n/v, 0) = 0$ for the nth order no-beam operating point and $\partial\Phi_n$ signifies the derivative evaluated at that point.

For purely spatial growth, the first term is neglected. The last term can be evaluated by the chain rule to yield

$$\frac{\partial\Phi_n}{\partial\omega_p^2}\omega_p^2 = \frac{\partial\Phi_n}{\partial\epsilon_\parallel}\frac{\partial\epsilon_\parallel}{\partial\omega_p^2}\omega_p^2 = -\frac{\partial\Phi_n}{\partial\epsilon_\parallel}\frac{\omega_p^2}{\gamma^3}\frac{1}{(\omega - k_z v)^2}. \tag{12}$$

The approximate dispersion relation therefore has a cubic form. This equation has three roots, one of which has a negative imaginary component implying exponential growth. Derivatives of the general case are intractable, but note that Φ is largely insensitive to electron beam thickness for $qa \gg 1$. The approximate spatial growth rate ($\alpha \equiv -\mathrm{Im}[k]$) in the wide beam limit ($a\to\infty$) is then

$$\alpha_n = \frac{\sqrt{3}}{2}\left(\frac{\omega_p}{\gamma v}\right)^3 \sqrt{\frac{v}{\omega_p \frac{\partial\Phi_n}{\partial k_z}}}. \tag{13}$$

The temporal growth rate can be derived in a similar manner and is related to the spatial rate by $\mathrm{Im}[\omega_n^{\mathrm{approx}}] = \alpha_n v_g$, where $v_g \equiv \sqrt[3]{v v_{gn}^2}$ is the effective group velocity and $v_{gn} = (\partial\Phi_n/\partial k_z)/(\partial\Phi_n/\partial\omega)$ is the group velocity of the no-beam mode at the nth operating point.

The derivative $\partial\Phi_n/\partial k_z$, plotted for the first three orders in Fig. 3, is nearly proportional to $1/(\beta - \beta_{\mathrm{th}})$, where β_{th}

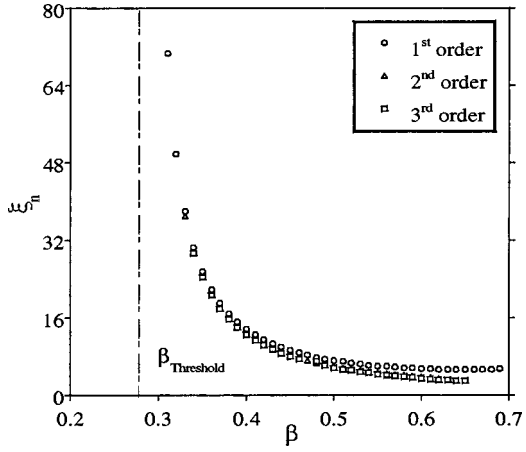

FIG. 3. The derivative $\xi_n = \partial\Phi_n/\partial(k_z d)$ calculated for GaAs ($\epsilon = 13.1$) with $g = 0$ at operating points defined by beam velocity. The first three orders are shown.

$= 1/\sqrt{\epsilon}$ is the Čerenkov threshold velocity. Assuming constant total current, independent of the accelerating voltage, then ω_p^2 is inversely proportional to β. The velocity at peak gain then satisfies

$$\beta_{\text{peak}}^3 + 2\beta_{\text{peak}} - 3\beta_{\text{th}} = 0, \tag{14}$$

which has an approximate solution

$$\beta_{\text{peak}} \approx \beta_{\text{th}}(3 - \beta_{\text{th}})/2. \tag{15}$$

This result yields slightly higher values than those calculated numerically.

If no gap exists ($g \to 0$), the derivative $\partial\Phi_n/\partial k_z$ is independent of order for $n > 1$, as shown in Fig. 3. Therefore, this approximation suggests that the gain is constant for increasing mode order as long as the gap is negligible.

This result is counterintuitive. The thickness of the interaction region is determined by the evanescent length ($1/q \propto 1/\omega$). The number of electrons participating in the gain process then shrinks with increasing frequency, assuming constant current density; and so one should expect gain to diminish for higher orders. This gain is constant for all orders in the face of the nearly universal rule that resonator efficiency drops as one moves to higher frequency.

IV. NUMERICAL RESULTS

The roots of the general dispersion equation (7) can be found numerically and the parametric gain dependence studied. A plot of the first three spatial gain orders is given in Fig. 4 with $g = 0$, $a \to \infty$. From the plot, it is clear that, with zero gap, the symmetry anticipated in the approximate formula holds generally. The shape of the gain curve is identical for each order and the peak gain value approach the asymptotic limit at high order. Note again that the plasma frequency is constant and the number of participating electrons drops inversely with the order.

We computed both spatial and temporal gain and found that they are related by $\text{Im}[\omega_n] = \alpha_n v_g$ where the group velocity is the slope of the real part of the dispersion curve. Also, gain is insensitive to electron beam thickness until the beam becomes narrower than the evanescent length ($qa < 1$), whereupon gain drops.

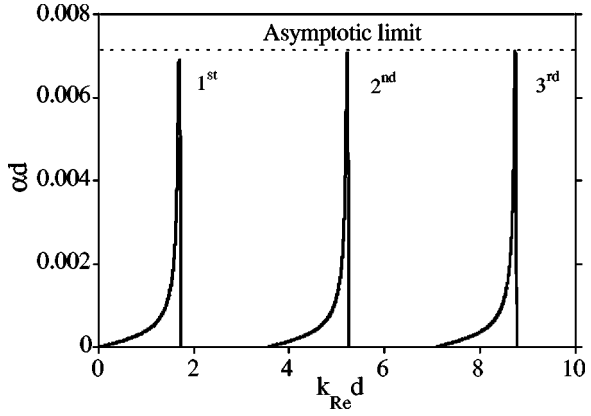

FIG. 4. Exact numerical spatial gain. The first three orders are shown with $g = 0$, $a \to \infty$, $\beta = 0.37$, $\omega_p d/c = 0.0018$, and $\epsilon = 13.1$. The asymptotic peak value for high orders is indicated.

With a finite gap, the gain is exponentially dependent on the ratio of the gap to the evanescent length. Therefore, the gap is negligible when it is small compared to this length ($q_o g \ll 1$). When viewing all orders together, the curve of peak gain is flat at low frequency and then rolls off as the evanescent length shrinks below the gap as shown in Fig. 5. The roll-off frequency is given, from the definition of q_o, by the relation

$$\omega_{\text{max}} g/\gamma v \approx 1. \tag{16}$$

Therefore, without considering practical limitations, the maximum achievable frequency is primarily determined by the beam energy and gap size.

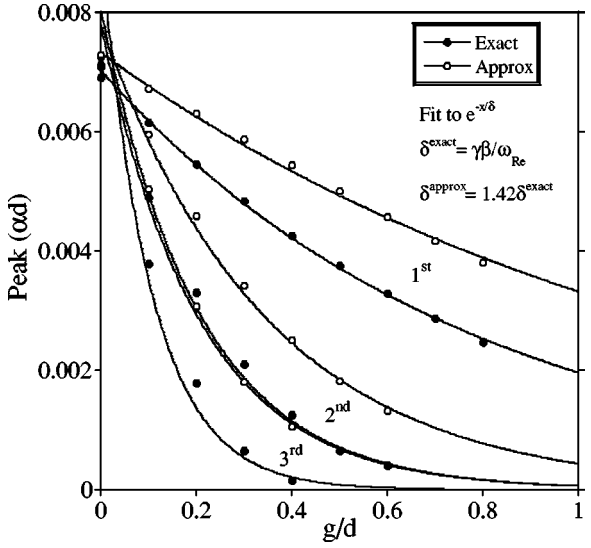

FIG. 5. Peak spatial gain with varying gap size and $\beta = 0.37$. Both exact (solid dots) and approximate (open circles) results are shown for the first three orders with fits to an exponential function. Note that the approximate result produces a 40% weaker gap dependence.

V. PRACTICAL CONSIDERATIONS

The gain in a free-electron laser (FEL) is limited by the quality of the driving electron beam. The primary characteristics quantifying beam quality are the emittance and the depth of field. The emittance ε is the product of the radius and angular spread of the beam. It can be reduced but not eliminated by accelerating the beam, and so is typically normalized to represent the quality of the source: $\varepsilon_N = \gamma\beta\varepsilon$. For particularly dense beams, Coulomb repulsion increases divergence and shortens the depth of field. The maximum current for an emittance limited beam of waist radius r_o is

$$I_{\max} = I_A(\gamma\beta)^3\varepsilon^2/2r_o^2, \tag{17}$$

where $I_A = mc^3/e = 17$ kA is the Alfvén current.

The depth of field is the axial range around the beam focus, over which its radius remains roughly constant and so determines the maximum interaction length of the CFEL. Defining the depth of field, where the beam area doubles compared to the waist, the range is

$$L = 2\gamma\beta r_o^2/\varepsilon_N. \tag{18}$$

In order for the device to produce coherent radiation, the total gain αL must be greater than unity. Including the above constraints in the approximate formula, Eq. (13) produces the inequality

$$\sqrt{3}e^{-g\omega/\gamma v}\left[\frac{2\gamma\beta r_o^2}{\varepsilon_N \partial\Phi_n(g=0)/\partial k_z}\right]^{1/3} \geqslant 1. \tag{19}$$

The inclusion of the finite gap dependence is justified in Fig. 5.

An experiment can be designed in either of the two ways. In one configuration, the required current can be minimized by tightly focusing the beam over the dielectric and extending the resonator length to the full depth of field L. The finite beam divergence angle limits the gap to $g \geqslant r_o/2$ so that the maximum frequency attainable by a CFEL in this configuration can be written, with Eq. (16), simply as

$$\nu_{\max} = \frac{\omega_{\max}}{2\pi} \approx \frac{0.2\gamma\beta c}{\sqrt{\varepsilon_N d\ \partial\Phi_n(g=0)/\partial(k_z d)}}. \tag{20}$$

Figure 2 implies that $\omega_{\max}$ increases with shrinking dielectric thickness and increasing beam energy, though the most compact device would operate at peak gain ($\beta = 0.37$ for GaAs). One version of the CFEL utilizes a scanning electron microscope generating a very high quality beam ($\varepsilon_N = 3 \times 10^{-8}\pi$ mrad) at low energies. Choosing a dielectric thickness of 50 μm, the smallest that can easily be machined, and $\beta = 0.37$, the maximum frequency is $\nu_{\max} \approx 4.8$ THz. Note that this result assumes single-pass operation. Resonant confinement by end mirrors effectively lengthens the interaction region and raises $\omega_{\max}$ by the number of passes to 3/2 power.

In the second configuration, the gap can be reduced by using a resonator that is short as compared to the beam depth of field. This scheme also raises the maximum frequency, but requires much greater total current to achieve comparable gain. In practice, the beam focus can be adjusted to maximize the operating frequency for the current available.

VI. CONCLUSION

In summary, both approximate and numerical results indicate that when the beam-dielectric gap is small compared to the evanescent length, the growth rate is independent of mode order, despite the higher frequency of the reduced number of participating electrons. The peak gain of each order drops as the field evanescent length shrinks below the gap size.

This conclusion is significant for maintaining that a narrow gap is a simpler task than squeezing the electron beam into a shrinking mode area. In addition, relatively large and robust resonators can be employed with a sufficiently small gap to achieve high frequency operation.

For optimum beam coupling, the gain rolloff defines a maximum operating frequency that depends only on the quality of the driving electron beam and the dielectric strength and thickness. This result implies a practical CFEL can operate as a coherent terahertz source.

ACKNOWLEDGMENTS

Support from ARO Grant No. DAAD19-99-0067 and NSF Grant No. ECS-0070491 is gratefully acknowledged.

[1] E.P. Garate and J.E. Walsh, IEEE Trans. Plasma Sci. **PS-13**, 524 (1985).

[2] J.E. Walsh, T.C. Marshall, and S.P. Schlesinger, Phys. Fluids **20**, 709 (1977).

[3] E. Fisch, A. Henning, and J.E. Walsh, IEEE J. Quantum Electronics **27**, 3 (1991).

[4] Y. Shibuya and T. Shiozawa, Trans. IEICE **E72**, 7 (1989).

[5] T. Shiozawa and H. Kondo, IEEE J. Quantum Electronics **QE-23**, 9 (1987).

[6] J.E. Walsh, in *Laser Handbook*, edited by W. Colson, C. Pellegrini, and A. Renieri (Elsevier Science, Amsterdam, 1990), Vol. 6, Chap. 14, pp. 497–500.